SOLID- AND GAS-SIDE RESISTANCES OF A SILICA-GEL DESICCANT WHEEL

RAMADAS NARAYANAN

Bibliographic citation

Narayanan, R. (2019). Solid- and gas-side resistances of a silica-gel desiccant wheel. *Energy Procedia, 160*, 139–146. https://doi.org/10.1016/j.egypro.2019.02.129

Link to Published Version: https://doi.org/10.1016/j.egypro.2019.02.129

Available online at www.sciencedirect.com

ScienceDirect

Energy Procedia 160 (2019) 139–146

Energy Procedia

www.elsevier.com/locate/procedia

2nd International Conference on Energy and Power, ICEP2018, 13–15 December 2018, Sydney, Australia

Solid- and gas-side resistances of a silica-gel desiccant wheel

Ramadas Narayanan *

Central Queensland University, 6 Univesity Drive, Bundaberg,Australia

Abstract

The operation of a solid desiccant evaporative cooling system largely depends on the dehumidification ability of the desiccant wheel and mathematical models are an effective tool to predict the transport behaviour of this wheel. A complete theoretical model would account for both the gas-side resistance, which is due to the convective heat and mass transfer between the air and the desiccant surface, and the solid-side resistance, which is caused by the diffusion of moisture and conduction of heat through the solid desiccant layer. A mathematical model is developed by deriving the partial differential equations of mass and energy balance of a representative channel the desiccant wheel moving through the supply and regeneration air streams in a 360° circular path. The effect of these resistances at different operating conditions on the performance of the wheel is rarely investigated. In this paper, two heat and mass transfer models are presented, the first one incorporating gas-side resistance and the second one includes both solid-side and gas-side resistances. The models are compared with experimental data. It can be concluded that the gas-side resistance is of considerably higher significance compared to the solid-side resistances.

Keywords: : Desiccant wheel; dehumidification; gas-side resistance; solid-side resistance

1. Introduction

The desiccant evaporative cooling system is a potential and eco-friendly alternative to energy-intensive vapour compression chillers [1-3]. They are actually a thermally driven on an open cycle cooling system with a combination

* Corresponding author. Tel.: +61 7 4150 7107; fax: +61 74150 7090.
E-mail address: r.narayanan@cqu.edu.au OR ramadas.n@gmail.com

1876-6102 © 2019 The Authors. Published by Elsevier Ltd.

10.1016/j.egypro.2019.02.129

of a desiccant wheel which is dehumidifier with the hygroscopic material, a heat recovery wheel, and evaporative coolers. At first, air is first dehumidified in the desiccant wheel to low humidity levels. Then it is cooled in in two stages with a sensible heat recovery wheel followed by the evaporative cooler.

As the success of the desiccant evaporative cooling system largely depends on the dehumidification performance of the desiccant wheel, often this wheel is considered the heart of this cooling system, A desiccant wheel uses a solid desiccant such as silica gel for dehumidification. The wheel matrix has several identical channels in the direction of the wheel's axis of rotation. The matrix supporting structure has a desiccant material coating on this surface. When the wheel rotates about its axis, two separate air streams, the supply air stream and the regeneration air stream passes through the top and bottom sections of the wheel. The supply air is dried by the desiccant, and hot regeneration air reactivates the desiccant to allow the continuous dehumidification process. The regeneration and supply air sides are separated by clapboard. The flow passage of air in a desiccant wheel is usually of sinusoidal shape. Usually, a desiccant wheel available commercially is as dehumidifying cassette consisting of a desiccant wheel, clapboard, wheel case and driving motor.

The desiccant wheel used for dehumidification is quite similar to those commonly employed in heat recovery, but it rotates at lower speeds (10-25 revolutions per hour (rph)) [4]. This rotational speed allows the desiccant to adsorb moisture and minimises the amount of heat carried over from the hot regeneration air into the supply.

Nomenclature

Y_g	Humidity ratio of air inside the control volume 1 (kg/kg)
T_g	Temperature of air inside the control volume 1 (K)
Y_d	Humidity ratio of air inside the control volume 2 (kg/kg)
T_d	Temperature of air inside the control volume 2 (K)
W_d	Water vapour content of desiccant (kg/kg)
ρ_g	Density of air (kg/m^3)
ρ_d	Density of desiccant (kg/m^3)
D_h	Hydraulic diameter (m)
Pi_n	Perimeter of the channel (m)
φ_d	Relative humidity of air in the control volume 2
cp_g	Isobaric specific heat capacity of air (J/kg/K)
cp_d	Specific heat capacity of desiccant (J/kg/K)
c_t	Combined specific heat capacity (J/kg/K)
α	Heat transfer coefficient (W/m^{2}K)
u_g	Velocity of supply air and regeneration air (m/s)
Da	Effective diffusion coefficient for ordinary and Knudsen diffusion
Ds	Surface diffusion coefficient
q_a	Heat of adsorption (J/Kg)
β	Mass transfer coefficient (kg/m^{2}K)

2. Transport mechanism in a desiccant wheel

The transport phenomena occurring in a desiccant wheel has been an area of interest to many researchers, and several studies are available. There are many physical processes are involved in the adsorption of water vapour into the hygroscopic matrix from the air which offers resistances to vapour transfer from the gas side to the solid phase. These heat and mass transfer resistances can be classified into two groups, namely, gas-side and solid-side resistances. Gas-side resistance is the resistance of the vapour transported from the bulk gas to the surface of the solid desiccant, whereas solid-side resistance is the resistance of the transport of the adsorbed molecules into the pore structure of the desiccant material from the surface of the desiccant [5-11]. Gas-side resistance is mainly due to convective heat and mass transfer between the air and the desiccant. Solid-side resistance is due to heat conduction and mass diffusion within the desiccant. The vapour can diffuse through pores of the desiccant in three different ways, namely, by ordinary diffusion, Knudsen diffusion, and surface diffusion. Usually, all these mass transfer mechanisms are represented using Fickian type expressions with different diffusion coefficients, D_o, D_k and D_s. These coefficients can be estimated by the following expressions [4]:

$$\mathrm{Do} = 1.758 \text{ x } 10^{-4} \frac{{T_d}^{1.685}}{P_a} \tag{1}$$

$$\mathrm{Ds} = \frac{1}{\zeta} \mathrm{Do} \quad \exp(-0.9740 \text{x } 10^{-3} \frac{q_a}{T_d}) \tag{2}$$

$$\mathrm{D_k} = 97 \text{ a} \quad \left(\frac{T_d}{M_1}\right)^{1/2} \tag{3}$$

with T_d being the temperature of desiccant (K), p_a is the atmospheric pressure, ζ is the tortuosity of the path of the pore, a is the pore radius, M_1 is the molecular weight of water and q_a is the heat of adsorption.

A large number of mathematical models have been developed to predict the heat and mass transfer behaviour in air dehumidification applications with rotary desiccant wheels, and a comprehensive literature review of all of these models was done by Ge et al. [12]. But there have only been a few investigations on the influence of solid-side resistance on performance. The first one was by San [13], and this study considered only the surface diffusion among the solid-side resistances, but the major processes (Knudsen and ordinary diffusions) were not considered. The effect of axial diffusion was studied by Sphaier et. al. by comparing the results for various aspects of the ratios and Biot numbers [15]. In this work, it was concluded that axial heat and mass diffusion was negligible in most cases, and was significant only for a thicker desiccant substrate with elevated thermal conductivity. However, the study did not include other parameters like the variation in flow velocity flow, rotational speed and regeneration temperature. Therefore, in this current work, to further investigate the effect of solid-side resistance, results are obtained for both models with different values of air velocity, rotational speed, and desiccant layer thickness and regeneration temperature.

3. Derivation of governing equations

The desiccant wheel can be considered as a set of identical axial channels coated with desiccant. When one-dimensional laminar air flow occurs through a desiccant wheel, each channel will have identical behaviour, and a theoretical model of a single channel will be able to predict the performance of the whole wheel. The partial differential equations that represent these transport mechanisms will be set up to describe a single desiccant-coated flow channel, traversing through the respective supply and regeneration air streams in a 360° circular path. Even though the heat and mass transfer within the wheel will be in all three dimensions, simplifications are needed to enable the analysis [5-6]. Consequently, the following assumptions are made. To investigate the significance of the two resistances categorised as gas-side and solid-side resistances, two different models, namely the gas-side resistance (GSR) model and the gas and solid-side resistance (GSSR), are developed.

3.1. Gas- and solid-side resistance model

As the name indicates, a gas-side resistance (GSR) model of the desiccant wheel considers only the convective resistance in the bulk flow and so the resistances due to heat conduction and mass diffusion in the wheel are neglected. The control volume is separated into two parts: one is the air passage, and the other one is the desiccant layer. Figure 1 shows a desiccant wheel and the computation/domain of the model. The governing equations can be derived by using the principle of the conservation of mass and heat in these control volumes [17]. All these equations will have a mass/energy storage term, the rate of mass/energy variation term and source terms which will differ according to the resistances included and the dimensions of the heat and mass transfer considered.

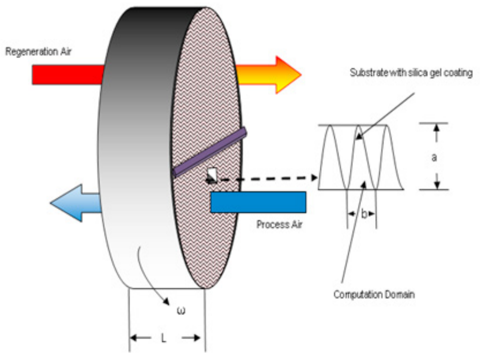

Fig 1. Desiccant wheel and computation domain of the model

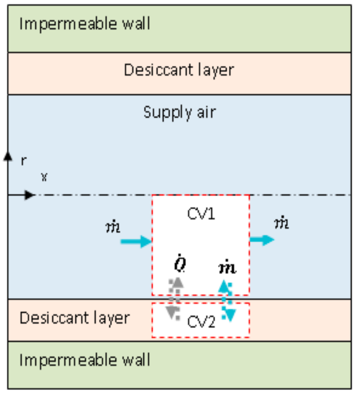

Fig 2. Channel cross-section with control volume for modelling

For the mathematical formulation of the problem, various assumptions are required. A channel of desiccant wheel is assumed sinusoidal and coated with silica gel, and the dehumidification and regeneration sections are of equal size. Various thermodynamic properties of the matrix such as thermal conductivity, heat and mass transfer coefficients and heat of adoption of silica gel are of the matrix is assumed to be constant. Also, conduction and mass diffusion in the air is negligibly small. The air flow within the channel is laminar as generally the hydraulic diameter of the channel is small, less than 5 mm and the velocity of flow is less than 3 m/s. The assumption of Lewis number as 1 makes the thermal and mass diffusivities equal.

A representative channel with the air control volume and desiccant control volume is shown in figure 2 is used for deriving the governing equations for the model. The control volume 1 (CV1) is in the air and control volume 2 (CV2) is in the desiccant. Based on the above assumptions, the mass and energy conservation equations can be derived. Here Y_g and Y_d represent the humidity ratio in CV1 and CV2, and T_g and T_d represent the temperature in these control volumes. W_d is the uptake of water which is the mass of water vapour adsorbed per unit mass of the desiccant.

With these assumptions, the mass and energy balance equations for the air and desiccant control volumes can be derived as given below.

The equation for the mass balance of CV1:

$$\frac{1}{u_g} * \frac{\partial Y_g}{\partial t} + \frac{\partial Y_g}{\partial x} = \frac{4\,\beta}{u_g\,D_h}\left(Y_d - Y_g\right) \tag{4}$$

The equation for the energy balance of CV1:

$$\frac{1}{u_g} * \frac{\partial T_g}{\partial t} + \frac{\partial T_g}{\partial x} = \frac{4\alpha}{u_g\,D_h\,c_{pg}}\left(T_d - T_g\right) \tag{5}$$

The equation for the mass balance of CV2:

$$\rho_g\,\frac{\partial Y_d}{\partial t} + \rho_d\,\frac{\partial W_d}{\partial t} = \rho_g\,\mathrm{D_a}\,\frac{\partial^2 Y_d}{\partial t^2} + \rho_d\,\mathrm{D_s}\,\frac{\partial^2 W_d}{\partial t^2} + \frac{\beta\rho_g P_{in}}{A_d}\left(Y_g - Y_d\right) \tag{6}$$

The equation for the energy balance of CV2:

$$\rho_d\,c_t\,\frac{\partial T_d}{\partial t} = \lambda_d\,\frac{\partial^2 T_d}{\partial x^2} + \frac{\alpha P_{in}}{A_d}\left(T_g - T_d\right) + q_a\rho_d\,\frac{\partial W_d}{\partial t} \tag{7}$$

Equations 4, 5, 6 and 7 will be the governing equations for the GSSR model.

3.2. Gas-side resistance model

For the gas-side resistance model, the solid-side resistances are neglected. So, the mass and energy balance equations (Equations 4 and 5) in CV1 remain the same, but the diffusive and conductive terms of Equations 6 and 7 will not be there. Therefore, the second and third terms in the right-hand side of Equation 6 and the first term in the right-hand side of Equation 7 will disappear, and the new equations will be as given below:

Mass balance in CV2:

$$\rho_g \frac{\partial Y_d}{\partial t} + \rho_d \frac{\partial W_d}{\partial t} = \frac{\beta \rho_g P_{in}}{A_d} (Y_g - Y_d) \tag{8}$$

Energy balance in CV2:

$$\rho_d \ c_t \frac{\partial T_d}{\partial t} = \frac{\alpha P_{in}}{A_d} (T_g - T_d) + q_a \rho_d \frac{\partial W_d}{\partial t} \tag{9}$$

Therefore, Equations 4, 5, 8 and 9 will form the governing equations for the GSR model.

3.3. Auxiliary Equations

It can be noticed that the governing equations have five unknown variables, Y_g, Y_d, W_d, T_g and T_d. To solve these simultaneous equations, one of the variables has to be eliminated. This can be done by relating the equilibrium humidity ratio of air, Y_d, to the water content, W_d, and the temperature of the desiccant, T_d. In this case, an equilibrium isotherm relationship of silica gel can be used as it shows the uptake of water vapour as a function of relative humidity of air which is a function of the humidity ratio and the temperature.

The equilibrium humidity content of regular density silica gel is governed by the following isotherm relationship [5]:

$$\varphi = 0.0078 - 0.05759 W_d + 24.16554 {W_d}^2 - 124.78 {W_d}^3 + 204.226 \, {W_d}^4 \tag{10}$$

where W_d is the water content, and

φ is the relative humidity of the air.

The heat of adsorption is determined by using the following expression [1]:

$$q_a = \begin{cases} -12400 W_d + 3500 & W_d \leq 0.05 \\ -1400 W_d + 2900 & W_d > 0.05 \end{cases} \tag{11}$$

Using psychrometric relationships, the relative humidity and humidity ratio are given below [2]:

$$\frac{\varphi}{Y_d} + 1.61\varphi = 10^{-6} e^{5294/T_d} \tag{12}$$

Since the channel geometry is assumed to be sinusoidal, the following expression can be used to calculate the hydraulic diameter [12]:

$$D_h = a \left[1.0542 - 0.466 * \left(\frac{a}{b}\right) - 0.1180 * \left(\frac{a}{b}\right)^2 + 0.1794 \left(\frac{a}{b}\right)^3 - 0.043 \left(\frac{a}{b}\right)^4 \right] \tag{13}$$

The convective heat and mass transfer coefficients can be calculated from the Nusselt number and the Lewis number respectively. For the sinusoidal-shaped channel, these coefficients can be calculated using the following expressions:

$$N_{uT} = 1.1791 \ (1 + 2.7701 \left(\frac{a}{b}\right) - 3.1901 \left(\frac{a}{b}\right)^2 - 1.9975 \left(\frac{a}{b}\right)^3 - 0.4966 \ \left(\frac{a}{b}\right)^4 \tag{14}$$

$$N_{uH} = 1.903\ (\ 1 + 0.455\left(\frac{a}{b}\right) + 1.2111\left(\frac{a}{b}\right)^2 - 16805\left(\frac{a}{b}\right)^3 - 0.7724\ \left(\frac{a}{b}\right)^4 - 0.1228\left(\frac{a}{b}\right)^5 \qquad (15)$$

$$N_u = (N_{uT} + N_{uH})/2 \qquad (16)$$

$$N_u = \frac{\alpha}{\lambda_a D_h} \qquad (17)$$

$$L_e = \frac{\alpha}{\rho_g \beta\, c_{pg}} \qquad (18)$$

3.4. Boundary and initial conditions

The initial and boundary conditions for the governing equations are given Table 1below. The wall boundaries are assumed as adiabatic and impermeable.

Table 1: Boundary and Initial conditions

For the supply air section		For the regeneration section
$Y_g(t,0) = Y_{g\ in}$		$Y_g(t,0) = Y_{g\ in1}$
$T_g(t,0) = T_{g\ in}$		$T_g(t,0) = T_{g\ in1}$
$T_d\,(0, x) = T_d\,(t_r, L-x)$		$T_d\,(0, x) = T_d\,(t_p, L-x)$
$W_d\,(0, x) = W_d\,(t_r, L-x)$.		$W_d\,(0, x) = W_d\,(t_p, L-x)$.

4. Results

The governing equations for the gas-side resistance (GSR) model and the gas and solid-side resistance (GSSR) model are solved using COMSOL Multiphysics which is finite element analysis, solver and simulation software for coupled partial differential equations. The inlet condition of the supply air used in this model is 0.0142 kg/kg dry air as humidity ratio and 35°C as the temperature. The reaeration temperature is 120° C, and the air velocity is 2m/s. Since the supply air and regeneration sections are assumed to be equal, angles for both sections will be 180°, and the ratio between the area of supply air section and regeneration air (SR ratio) is 0.5.

The validation of the two numerical models is shown in Figures 3 and 4 by plotting the outlet humidity ratio and temperature results for a revolution of the wheel and its comparison with Brillhart's experimental results [16]. It can be observed that the model has good agreement with the experimental outlet humidity ratio and temperature. As in the case of previous theoretical studies [17-19], the deviation of the humidity ratio curve from the experimental value can be attributed to greater experimental uncertainties at the beginning of the dehumidification period. The figures also demonstrate that, at the selected operating conditions, the effect of solid-side resistance is negligible.

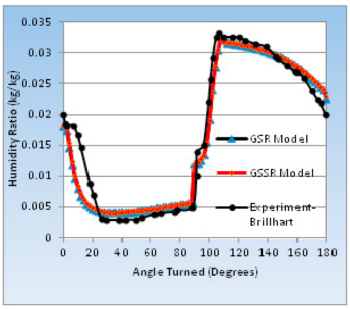

Fig 3. Comparison of humidity ratio with Brillhart's Experimental results

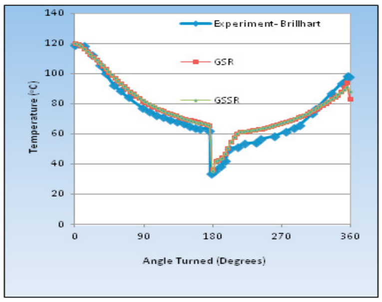

Fig 4. Comparison of temperature results with Brillhart's experimental results

5. Comparison of models

Figures 5 and 6 show the variations in the outlet humidity ratio and temperature of the GSR and GSSR models for different input values of velocity during the dehumidification process. The velocity values are varied between 2 m/s and 3 m/s. At 2 m/s, the outlet humidity ratios of both GSR and GSSR models follow closely, but at the higher value velocity, there is a large difference between the profiles. The temperature profiles for both models are close to each other at a velocity of 3 m/s, whereas there is only a slight variation at the lower velocity.

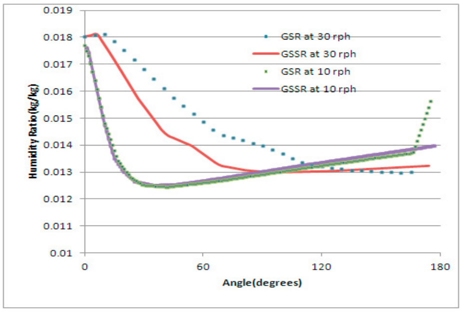

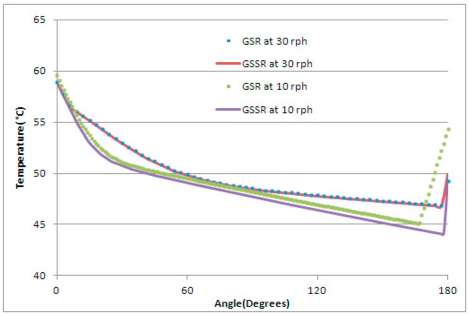

Fig 5. GSR and GSSR model outlet humidity ratio results at different velocities

Fig 6. GSR and GSSR model outlet temperature for different velocities

Figure 7 and 8 shows the outlet humidity ratio and temperature profiles for the GSR and GSSR models at rotational speeds 10 and 30 rph. In these cases, there is a significant deviation between both models' humidity ratio profiles particularly at 30rph, but the temperature profiles match closely.

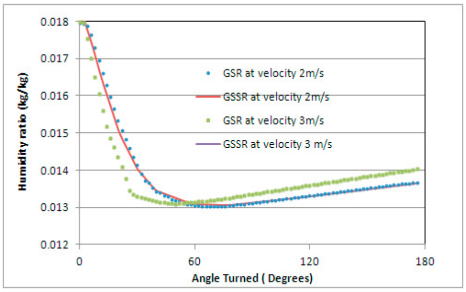

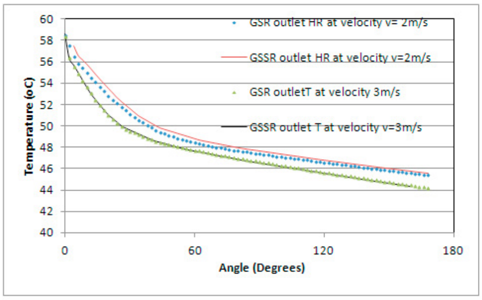

Fig 7. GSR and GSSR model HR at different rotational speeds

Fig 8. GSR and GSSR model temperature at different rotational speeds

When the thickness of the desiccant layer is changed to 0.25 mm from 0.15 mm, there is no significant difference between the two models' results, but when a thickness of 0.35 mm is used, there is a significant deviation between the GSR and GSSR models as shown in Figures 8 and 9.

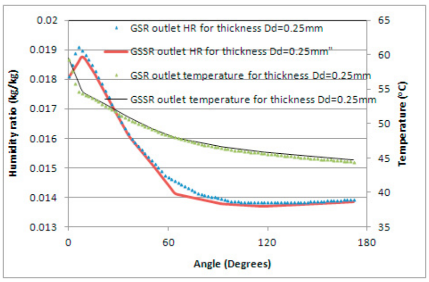

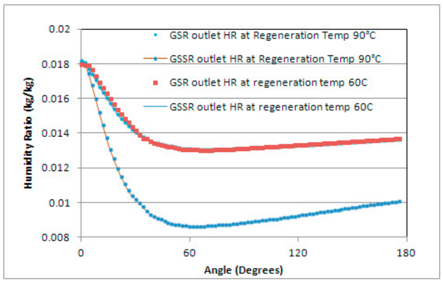

Fig 9. GSR and GSSR model results for desiccant layer thickness 0f 0.25 mm

Fig 10. GSR and GSSR model results for desiccant layer thickness of 0.35 mm

The GSR and GSSR models do not show much difference when the regeneration temperature is changed which is indicated in Figure 11 and 12.

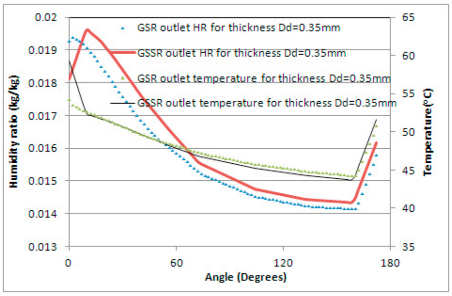

Fig 11. GSR and GSSR model HR at different Regeneration temperatures

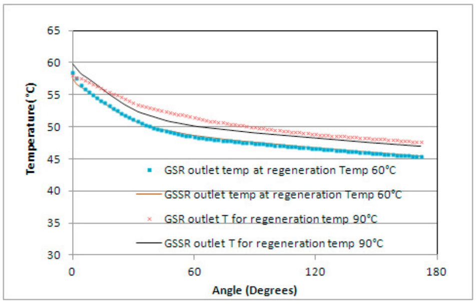

Fig 12. GSR and GSSR model temperature at different regeneration temperatures

6. Conclusions

The two numerical models of a counter flow desiccant wheel, the GSR and GSSR models were developed and the results have been compared with published experimental data, which showed close agreement. The variation of all the output parameters was analysed and discussed. The two models were used to investigate the relative importance of solid-side resistances and gas-side resistances, and it was found that the GSR model gave reasonably accurate results for most of the cases and both models gave almost identical results. However, at different rotational speeds, velocities of flow and thicknesses of the desiccant layer, there was some variation between the models, which showed the significance of solid-side resistance in these cases.

References

[1] Henning, H-M. "Solar assisted air conditioning of buildings – an overview." *Applied Thermal Engineering*, **27**(10)(2007):. 1734-1749.
[2] Narayanan, R. "Heat-Driven Cooling Technologies." in *Clean Energy for Sustainable Development: Comparisons and Contrasts of New Approaches* (2017):191-212. London, UK. Elsevier.
[3] Narayanan, R., Halawa, E. and Jain, S. "Performance Characteristics of Solid-Desiccant Evaporative Cooling Systems." *Energies 11*(10) (2018): 2574.
[4] Zhang, L.Z. and J.L. Niu. "Performance comparisons of desiccant wheels for air dehumidification and enthalpy recovery." *Applied Thermal Engineering* 2002. 22(12): p. 1347-1367.
[5] Pesaran, A.A. "Moisture Transport in Silica Gel Particle Beds." PhD Thesis (1983), University of California, Los Angeles.
[6] Narayanan, R., Saman W.Y, White S.D., and Goldsworthy M. "Comparative study of different desiccant wheel designs." *Applied Thermal Engineering* 31(10) (2011):1613-1620.
[7] Narayanan,R. "Development of a Thermally-driven Solid Desiccant System for Dehumidification /Cooling." PhD Thesis (2012), University of South Australia.
[8] Narayanan R., Saman W.Y., White S.D. and Goldsworthy M. "A Non-Adiabatic Desiccant wheel: Modelling and experimental validation." *Applied Thermal Engineering* 61(2) (2013) :178-185.
[9] Narayanan, R. "Theoretical modelling of silica gel desiccant wheels." *Applied Mechanics and Materials*, vol. 787, (2016):311-317.
[10] Narayanan R., Saman W.Y, White S.D. and Goldsworthy M. "Modelling and Parametric Analysis of Silica-gel Desiccant Wheels." *Proceedings of International Institute of Refrigeration Gustav Lorentzen Conference* (2010), Sydney.
[11] Narayanan, R. "Investigation of geometry effects of channels of a silica-gel desiccant wheel", *Energy Procedia, 2017,110* (pp. 20-25).
[12] Ge, T.S., Li Y. Wang R.Z. and Dai, Y.J. "A review of the mathematical models for predicting rotary desiccant wheel." *Renewable and Sustainable Energy Reviews* 12(6) (2008):1485-1528.
[13] San, J.Y. "Heat and mass transfer in a two-dimensional cross-flow regenerator with a solid conduction effect." *International Journal of Heat and Mass Transfer* 36(3)(1993): 633-643.
[14] Sphaier, L.A. and W.M. Worek "The effect of axial diffusion in desiccant and enthalpy wheels." *International Journal of Heat and Mass Transfer* 49(7-8)(2006): 1412-1419.
[15] Ruivo, C.R., Costa J.J. and Figueiredo A.R. "On the behaviour of hygroscopic wheels: Part I – channel modelling." *International Journal of Heat and Mass Transfer* 50(23-24) (2007): 4812-4822.
[16] Brillhart, P.L. "Evaluation of Desiccant Rotor Matrices using Advanced Fixed Bed System." *PhD Thesis* (1997), Illinois University, Chicago.
[17] Chung, J.D., Lee, D.Y. and Yoon, S.M. "Optimisation of desiccant wheel speed and area ratio of regeneration to dehumidification as a function of regeneration temperature". *Solar Energy*, 83(5)(2009): 625-635.
[18] Ali, M., Vukovic V., Sahir M. H. and Basciotti D. "Development and validation of a desiccant wheel model calibrated under transient operating conditions." *Applied Thermal Engineering* 61(2) (2013): 469-480.
[19] Bareschino, P., Diglio G., Pepe F., Angrisani G., Roselli C. and Sasso, M."Modelling of a rotary desiccant wheel: Numerical validation of a Variable Properties Model." *Applied Thermal Engineering* 78 (2015): 640-648.